

Performance of NiCrAlY Coatings Deposited by Oxyfuel Thermal Spraying in High Temperature Chlorine Environment

K.A. Habib, M.S. Damra, J.J. Carpio, I. Cervera, and J.J. Saura

(Submitted April 7, 2014; in revised form June 9, 2014; published online July 24, 2014)

A microcrystalline Ni-22Cr-10Al-1Y (wt.%) coating was deposited on AISI 304 stainless steel by the oxyfuel thermal spray technique. The deposited coating was subjected to heat treatment to improve the microstructure characteristics and its corresponding high-temperature properties. The isothermal high-temperature corrosion behavior at 650 and 700 °C in synthetic air and in the presence of 1% Cl₂ was investigated using thermogravimetric analysis, x-ray diffraction, and scanning electron microscopy with energy-dispersive x-ray spectroscopy. The results indicated that the deposited NiCrAlY coating possessed acceptable oxidation-corrosion resistance at 650 °C owing to the formation of extensive amounts of the protective oxide of Cr₂O₃; NiO and a lesser amount of a Cr_{1.12} Ni_{2.88} metallic phase are also formed. At 700 °C, the coating lost its protective characteristic because of the excessive consumption of thermodynamically stable phases by oxidation-chlorination process. In this case, the steel base and the coating were attacked by chlorine during the exposure time; the mass gain of the NiCrAlY coating was slightly higher and provided only a limited protection up to 11 h; thereafter, breakdown of the layer of oxides occurred and this is attributed to the formation of non-protective oxides mainly β-Fe₂O₃ and Fe_{21.33}O₃₂ and the depletion of chromium.

Keywords high-temperature degradation, NiCrAlY coating, oxy-chlorination, oxyfuel thermal spray technique

1. Introduction

Several technological problems appear in power plants using bio-mass and municipal waste as fuel. These include high temperature corrosion via penetration of corrosive gases through the scale and/or corrosion and erosion of underlying substrate via corrosive salts. Solutions to these problems on low cost substrate materials in combination with tailored coating become technically and economically attractive (Ref 1).

MCrAlY coating (M = Ni or/and Co) deposited by thermal spraying techniques is widely used in the petroleum sector, in components of industrial gas turbines and aircraft engines and in other applications in which high thermal and mechanical loads have to be supported. The protective feature is so important that about 75% of all hot components in industrial and aircraft engines are coated (Ref 2, 3). Due to the requirement of enhanced power-out of energy plants (Ref 4), there is urgent demand for stable MCrAlY coating with improved long-term performance, as the inlet temperature is increased.

The good protection against high-temperature oxidation and corrosion provided by MCrAlY overlays is attributed to the

formation of dense and adherent alumina and/or chromia scales (Ref 5, 6). These coatings involve the formation at high temperatures of protective Cr₂O₃ and Al₂O₃; the protective effect of Cr₂O₃ is limited to around 1000 °C, as volatile CrO₃ is formed at this temperature, whereas protection by Al₂O₃ is effective at higher temperatures (Ref 7, 8).

Adding chromium and/or nickel to iron improves the alloy's resistance to chlorination attack. For this, nickel and nickel-based alloys and coatings are widely used in chlorine-containing environments. Such coatings offer protection not only against oxygen and nitrogen from the intake air environment but also to a certain extent against attack by fuel or air impurities, such as sulfur (SO₂ or SO₃), chlorine (from maritime and combustion environments), and liquid deposits (sulfates) (Ref 9).

Despite the homogeneous nature of thermally sprayed MCrAlY coatings, they always contain some oxides and porosity at splat boundaries (Ref 10, 11) which form an interconnected network through the whole coating (Ref 12).

High-temperature corrosion caused by combustion environments is usually accelerated by hot corrosion and gaseous aggressive species such as chlorine and sulfur in combination with oxygen. In oxidizing environments, chlorine accelerates oxidation by mechanism of active oxidation (Ref 13, 14). If active oxidation occurs, even small amounts of chlorine circulating through the coatings may cause severe damage to coatings themselves and especially may reduce the bonding strength of the coatings. On the other hand, if the transport of chlorine compounds through coatings is slow, the coatings might maintain their shielding capability.

In Cl₂ environment, the partial pressure of Cl₂ may be significant near oxides layer (Ref 11). Therefore, solid and

K.A. Habib, M.S. Damra, J.J. Carpio, I. Cervera, and J.J. Saura, Industrial Systems Engineering and Design, University JAUME I, Castellón, Spain. Contact e-mail: razzaq@esid.uji.es.

gaseous metal chlorides can be formed according to the reaction $M(s) + x/2 Cl_2(g) \rightarrow MCl_x(s, g)$. A comparison of the Gibbs free energies of formation for the different divalent chlorides at 600 °C shows the highest negative values for $CrCl_2$ (−286.0 kJ/mol) followed by $FeCl_2$ (−232.1 kJ/mol) and $NiCl_2$ (−174.2 kJ/mol) (Ref 15). The energies are very negative, so metals will react with chlorine and according to these data a less reactive behavior is expected for nickel than for iron and chromium. The solid chlorides formed have considerable equilibrium vapor pressures $p_v(Me_xCl_y)$ and evaporate continuously according to the following equation: $MCl_x(s) \rightarrow MCl_x(g)$. Metal chlorides can be formed leading to extreme corrosion rates owing to porous non-protective oxide scales and a spongy metal subsurface zone by selective “leaching” of alloying elements (Ref 9).

The formation of oxides and spinel of nickel, aluminum, and chromium contributed to the development of high temperature corrosion resistance of this coating. However, better understanding of the high temperature corrosion performance of such coating is needed in order to establish the mechanism of high temperature corrosion in the aggressive environments.

In previous works (Ref 16, 17), the effectiveness of OF thermal spray technique to improve the tribological behavior and oxidation protection of stainless steels at 850 °C was proven with a coating system composed of a Ni-Al alloy bond coat and a ceramic topcoat. In a more recent work (Ref 18), it was shown that NiCrAlY thermally sprayed by the OF thermal spray technique provides good oxidation resistance to AISI 304 and AISI 316 stainless steels for temperatures as high as 1000 °C for 50 h.

The aim of this work was to study the high-temperature corrosion behavior of NiCrAlY coatings deposited by the oxyfuel (OF) thermal spray technique exposed to an oxidation-chlorination environment. The analysis includes environmental conditions needed to form protective layers and the conditions that can cause breakdown of oxides layers in an oxidation-chlorination atmosphere. The oxides growth at the two studied temperatures is studied in order to get a better understanding of the oxidation-chlorination behavior.

2. Experimental Procedure

AISI 304 stainless steel, specimens of $20 \times 10 \times 1.2$ mm³, was used as substrates. Specimens were grit blasted with corundum particle of 99.6 wt.% purity and 0.53-mm mean particle size, using an air pressure of 0.4 MPa, incidence angle of approximately 45°, and a gun-to-substrate distance of 130 mm. The surface was then cleaned and degreased using acetone within an ultrasonic bath. The average surface roughness was 5.1 ± 0.5 μm and the mean roughness depth, defined as the vertical distance between the highest peak and deepest valley, was 28.3 ± 2.4 μm.

A commercially available Ni-22Cr-10Al-1Y powder produced by Praxair Surface Technologies-TAFA (Ni-343) with an average particle size of 28 μm was deposited on all the sample faces by a Castodyn CDS-8000 flame spray gun made by

Castolin Eutectic, with particles velocity around 300 m/s and maximum temperature of 3200 °C. Table 1 shows the parameters of the thermal spraying process.

Preparation of the top surface of the NiCrAlY coatings samples was achieved by grinding it with 240, 400, and 800 grade SiC in that order to obtain a flat and smooth surface; and finally was ultrasonically cleaned with acetone for 15 min.

Prior to the oxidation-chlorination test, the NiCrAlY-coated specimens were subjected to a heat treatment at 1100 °C for 4 h as detailed in Ref 18 to improve the microstructure of the coatings by reducing the porosity and therefore increasing the oxidation resistance.

Isothermal tests at 650 and 700 °C were performed on NiCrAlY-coated specimens. Samples were heated in a thermobalance (TGA 92-16, Setaram) using synthetic air plus 1% Cl_2 from room temperature to 650 and 700 °C at a rate of 40 K/min. They were maintained at these temperatures for 24 h and then cooled to room temperature at 40 K/min.

The OF thermally sprayed coatings were characterized using x-ray diffraction (XRD) and scanning electron microscopy (SEM) with energy-dispersive x-ray spectroscopy (EDS).

3. Results and Discussion

3.1 Thermogravimetry Experiments on NiCrAlY at 650 and 700 °C

Figure 1 shows that after 24 h at 650 °C the plot of the weight gain per unit area $\Delta W/S$ versus time (t) assumed a parabolic shape with a rate constant of 2.809×10^{-5} [$mg^2 \cdot (mm^{-4} \cdot s^{-1})$], calculated according to the equation:

$$(\Delta W/S)^2 = k_p t. \quad (\text{Eq 1})$$

At this temperature, the weight gain (oxidation rate) is relatively low and no sharp changes in the oxidation course can be observed after 24 h; at the end of the test, no external signs of corrosion damage (spallation and cracks) were observed on the surface of the specimen.

At 700 °C, the corrosion kinetics obeys a parabolic law in the initial stage because the weight gain due to oxidation is the dominant process; after 11 h, a second stage occurs, where the behavior becomes linear because oxides formed cannot afford enough protection because the chlorination process occurs (Ref 19). At this temperature, corrosion proceeds in two stages: an incubation period exhibiting a low corrosion rate, followed by accelerated corrosion attack. The incubation period is related to the formation of a protective oxide scale. Initiation of accelerated corrosion attack is believed to be related to the breakdown of the protective oxide scale.

3.2 XRD Analysis of NiCrAlY Coatings at 650 and 700 °C

The XRD patterns obtained from the surface of the OF thermally sprayed NiCrAlY sample after 24 h at 650 °C

Table 1 Parameters of thermal spray process

Sample	Preheating strokes	Distance (mm)	NiCrAlY coat strokes	Coat thickness (average) (μm)	Comp. air pressure Bar	Flame condition
AISI 304	1.2	150	9	186.5	3	Neutral

(Fig. 2) give evidence of the presence of stable Cr_2O_3 , NiO phases and $\text{Cr}_{1.12}\text{Ni}_{2.88}$ metallic phase.

After 11 h at 700 °C, surface products were identified by XRD. The major phases observed are as follows: $\text{Fe}_{21.33}\text{O}_{32}$, $\text{Cr}_{1.3}\text{Fe}_{0.7}\text{O}_3$, $(\text{Fe}_{0.6}\text{Cr}_{0.4})_2\text{O}_3$ in the oxidized coating, as well as minor peaks relative to $\beta\text{-Fe}_2\text{O}_3$ and AlFeO_3 phases (Fig. 3). The presence of iron in all phases formed indicates that Fe ions have diffused through the entire coating from the substrate base metal.

3.3 SEM Surface Analysis

The surface morphology of the coating after oxidation-chlorination at 650 °C for 24 h is presented in Fig. 4. From Fig. 4(a), it can be seen that no cracks or spallation of the oxide scales of the NiCrAlY coating after exposure have occurred. As can be seen from Fig. 4(b) and a corroborated by EDS analysis, three main phases were formed at this temperature (1) a lighter dispersed phase in the form of dotted blocky nodules with a

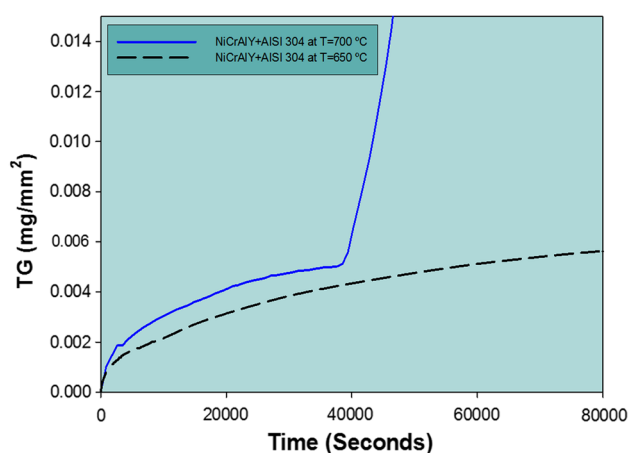


Fig. 1 Isothermal corrosion test of flame thermal sprayed NiCrAlY coat deposited on AISI 304 stainless steel at 650 and 700 °C in 1% Cl_2 environment for 24 and 11 h, respectively

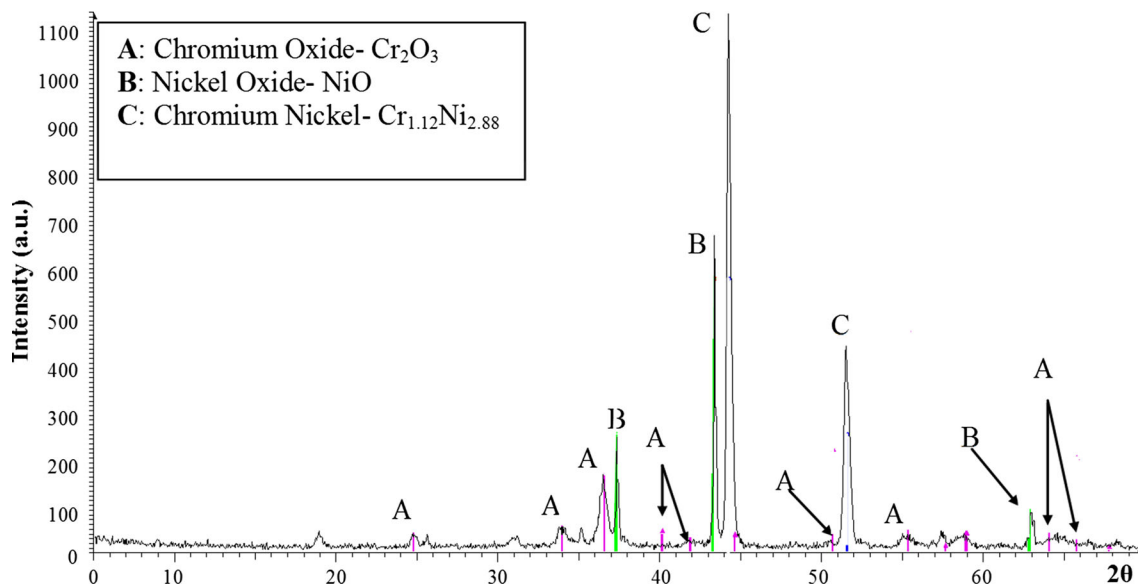


Fig. 2 XRD pattern of NiCrAlY deposited on AISI 304 stainless steel oxidized in Cl_2 environment at 650 °C for 24 h

composition (wt.%) of 72.96% Ni, 22.40% O, 4.54% Cr, 0.17% Al, and 0.19% Cl; (2) a darker phase in the form of spherical blocks with a composition of 49.58% Cr, 24.85% O, 19.81% Cl, 4.76% Ni, 0.64% Al, and 0.36% Y; and (3) extensive gray zones with a mean composition of 30.77% Ni, 30.77% O, 26.96% Cr, 11.07% Al, 0.35% Y, and 0.07% Cl.

SEM micrographs showing the surface morphology of the coating are depicted in Fig. 5. The micrographs indicate typical splats morphology for all deposited coating after 24 h at 700 °C; cracks and spallation of the oxide scales are observed. It can also be seen that microstructure of the coating is formed by a combination of ridges and nodules, (Fig. 5b, c, and d) and that between the nodules, there are smooth patches with clearly marked cracks on the surface. The presence of these cracks could explain how chlorine and oxygen directly accessed the substrate metal.

EDS analysis of the phase in the upper part of Fig. 5(b) gives the following elemental composition (wt.%): 18.1% O, 8.3% Cl, 24.58% Fe, 0.67% Al, 34.35% Cr, and 4% Ni; these results revealed the degradation of the NiCrAlY coating. Figure 5(d) shows a magnification of this zone which has a general elemental composition of 52.05% Cr, 30.44% O, 11.46% Fe, 3.29% Cl, 1.56% Ni, and 1.2% Al. Figure 5(e) shows a nodule of NiCrAlY coating; a punctual analysis of this part indicates the following elemental composition: 34.08% Cr, 33.32% Fe, 30.38% O, 1.31 Cl, and 0.77% Ni. The morphology of the nodule is tetragonal as seen in Fig. 5(f). The high content of Fe and O confirms the results obtained by XRD (no protective iron oxides have been formed).

3.4 Cross-Section Analysis

Figure 6 shows a general SEM image of the cross-section of the NiCrAlY deposited on AISI 304 stainless steel after exposure to synthetic air plus 1% Cl_2 at 650 °C for 24 h. EDS analysis shows that the main elements present (wt.%) are O (29%), Cr (22.41%), Al (10.5%), and Ni (32.4%) and a very low amount of Cl (0.52%) and Fe (0.08%). The presence of the main elements could confirm that protective oxides have formed, as shown from XRD results

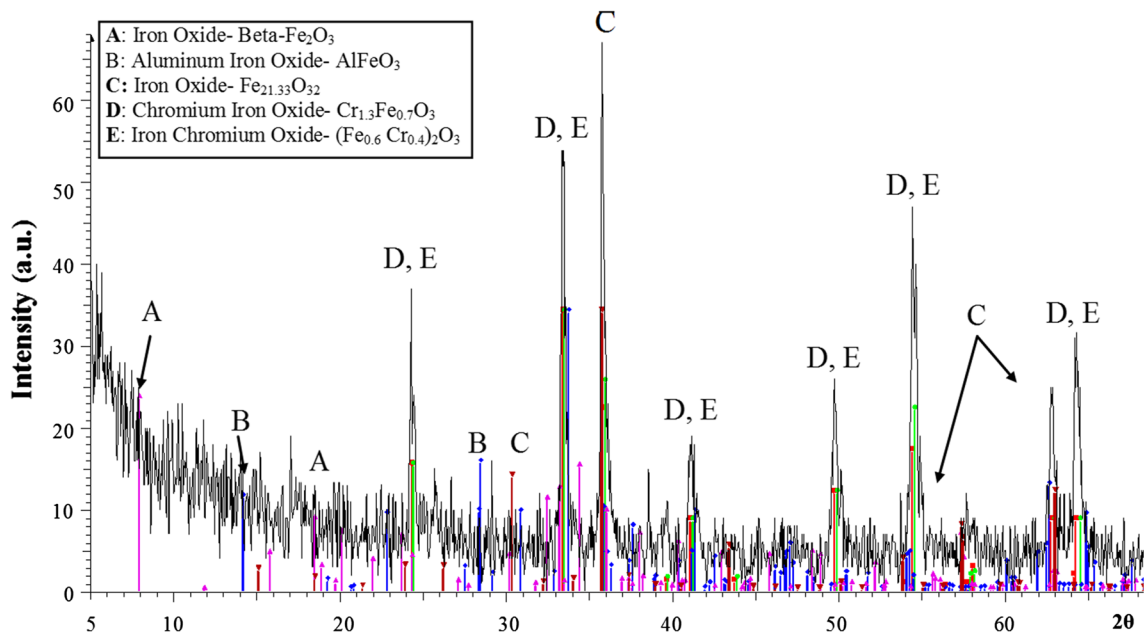


Fig. 3 XRD pattern for NiCrAlY deposited on AISI 304 stainless steel oxidized in Cl_2 environment at $700\text{ }^\circ\text{C}$ for 11 h

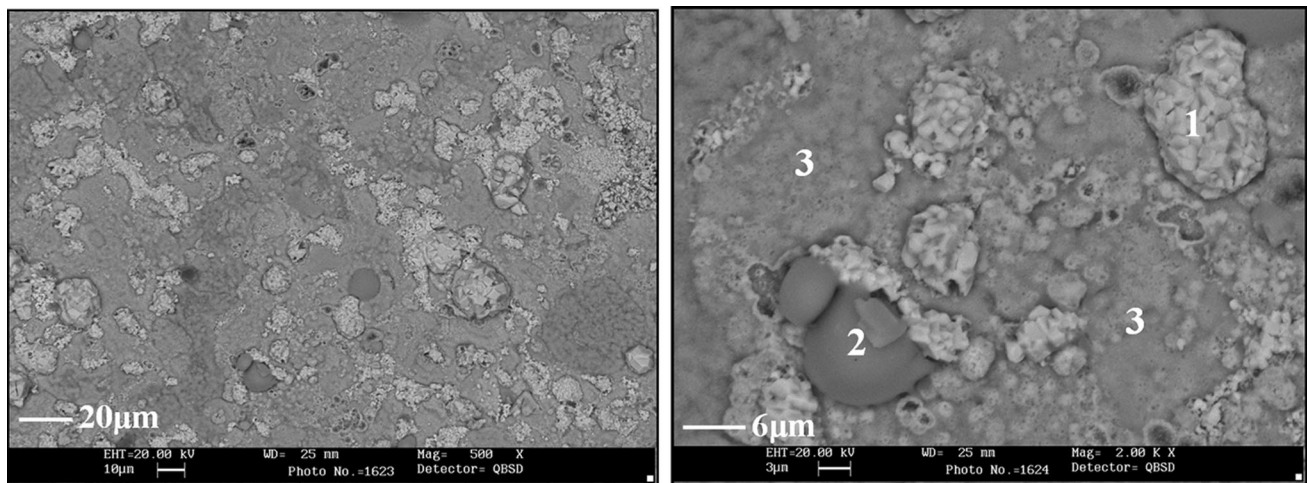


Fig. 4 SEM surface morphology of NiCrAlY coating after oxidation at $650\text{ }^\circ\text{C}$ in 1% Cl_2

From XRD results, only protective oxides products were detected at the surface of the coating. Neither internal attack of the coating nor attack on the substrate base metal was observed.

Figure 7 shows that the oxide top layer present on the NiCrAlY coating at $650\text{ }^\circ\text{C}$ consisted of two different overlying films (duplex oxide scale); the chemical composition of the inner film scale identified by EDS (wt.%) was 46.09% O, 40.46% Al, 9.42% Ni, and 4.04% Cr. The analysis of the outer scale indicated that drastic consumption of aluminum (14.74%) and enrichment of nickel (22.41) and chromium (22%) occurred; the proportion of oxygen detected was 40.85%. The high aluminum content in the coating is the reason not only for the formation of protective Al_2O_3 near the surface of the coating, but also the formation of Ni-Cr rich oxide on the surface that could be formed during the very beginning of the exposure at high temperature. The Al_2O_3 scale was established beneath the initially formed Ni-Cr rich oxide, which usually called transient oxide.

The SEM micrograph and elementals mapping of a cross-section of the oxidized specimen at $650\text{ }^\circ\text{C}$ after 24 h, (Fig. 8), show that the coating was able to stop the attack of chlorine because of the encircled and interconnected Al_2O_3 and Cr_2O_3 , (dark zones in the micrograph) network surrounding the boundaries of Cr-Ni metallic splats (light zones in the micrograph). The EDS mappings from the cross-section are consistent with the results obtained from XRD superficial analysis which showed that scale is formed by NiO, protective Cr_2O_3 , and the $\text{Cr}_{1.12}\text{Ni}_{2.88}$ metallic phase.

The Al_2O_3 phase surrounding Cr-Ni metallic splats is responsible for improving the oxidation resistance of the coating, because the formation of Al_2O_3 can hinder the diffusion of nickel and chromium from inside the splat to the surface and thus prevent the growth of Cr_2O_3 and NiCr_2O_4 , which is attributed to the low diffusion coefficients of nickel and chromium along the grain boundary of the metallic phase: the diffusion coefficient of aluminum along the grain boundary

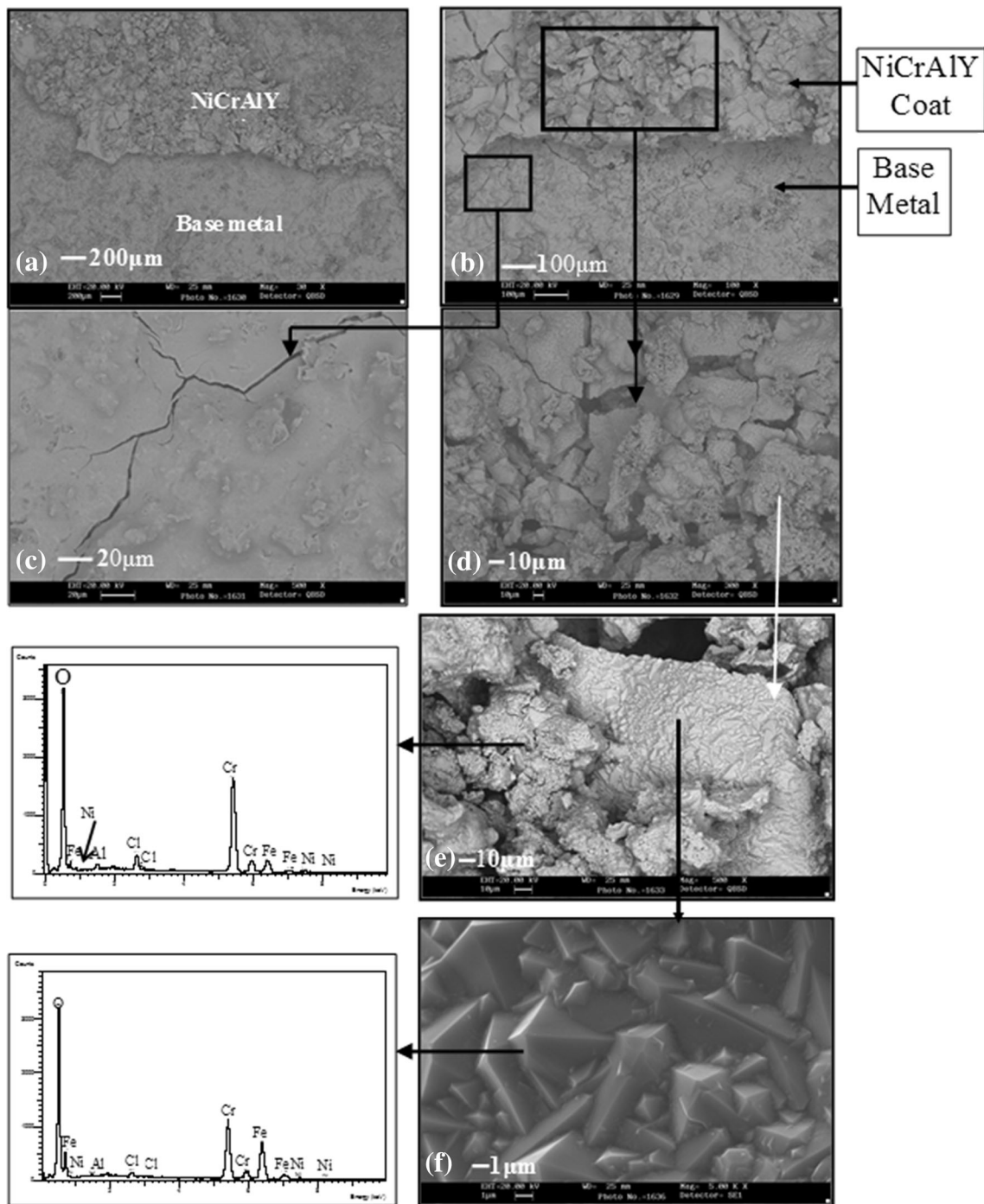


Fig. 5 SEM micrographs with EDS analysis of NiCrAlY deposited on AISI 304 after 11 h at 700 °C, showing surface morphology and composition at different locations

of nickel and chromium is greater than that of nickel and chromium (Al: $2.8 \times 10^{-4} \text{ m}^2/\text{s}$, Cr: $6.9 \times 10^{-11} \text{ m}^2/\text{s}$; Ni: $2.53 \times 10^{-10} \text{ m}^2/\text{s}$) (Ref 20). The formation of Al_2O_3 during oxidation-chlorination process can hinder the growth of the grains of the coatings during crystallization because it covers the grain boundary. The previous discussion leads us to state that the performance of the OF thermally sprayed NiCrAlY coating on austenitic stainless steel in an air plus Cl_2 atmosphere at 650 °C was good owing to the formation of this continuous chromium and aluminum-rich oxide double

layer of approximately 2- μm thick and the internal oxidation of the coating.

Figure 9 shows the SEM images and EDS analysis (elemental chemical composition) of the cross-section of the NiCrAlY-coated sample oxidized until the breakdown happened at 700 °C. It seems that the coat was strongly damaged and the corrosion spread toward the base metal. The NiCrAlY coating was penetrated by chlorine via splats boundaries, and was massively attacked; causing many cracks and interfaces between the base metal and the corrosion products layer. In

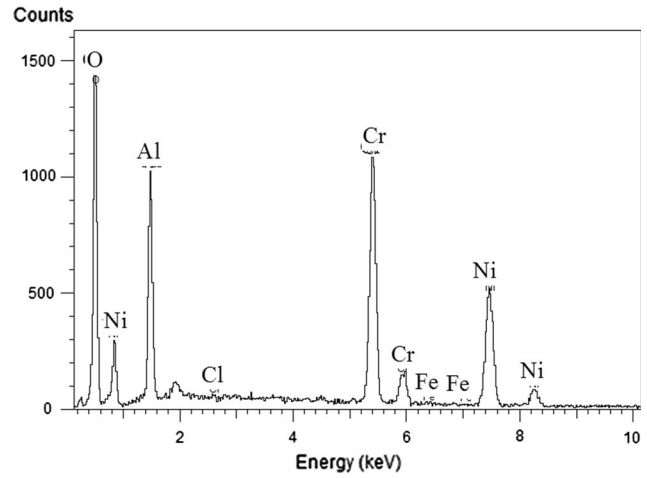
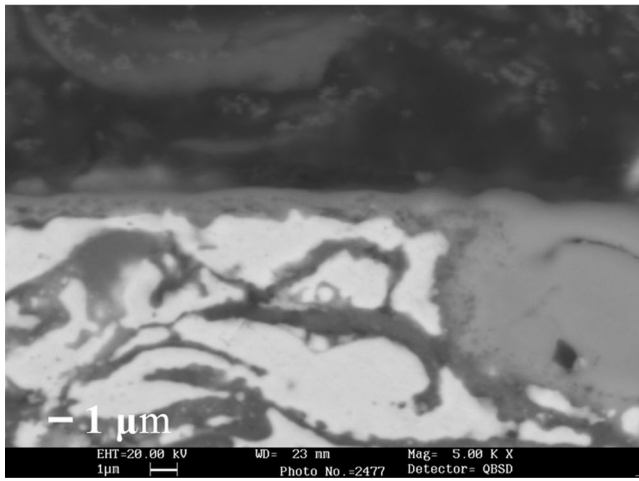


Fig. 6 SEM micrograph with EDS analysis of the cross-section of NiCrAlY coat deposited on AISI 304 corroded at 650 °C in 1% Cl₂ during 24 h

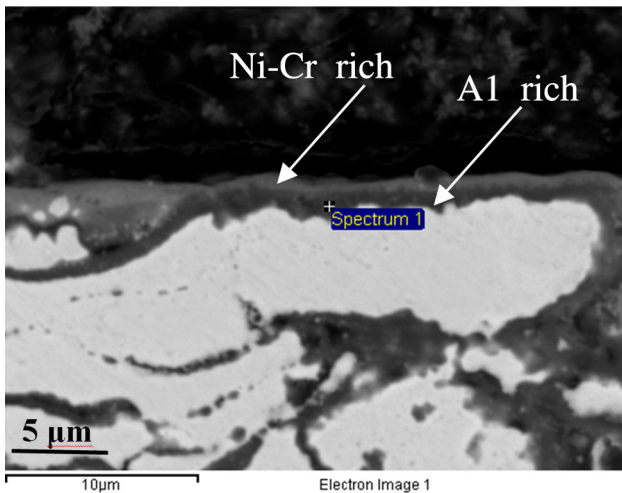


Fig. 7 Cross-section of duplex scale formed on the top of oxidized NiCrAlY coating after 24 h at 650 °C

Fig. 9(a), it seems that the metal substrate has been reached by chlorine and oxygen as can be deduced from the EDS analysis which shows chlorine content as high as 30% and an oxygen content of 23.65%. Figure 9(b) illustrates the morphology of the corrosion layer formed in the metal-coating interface, which is porous and severely cracked; EDS analysis showed that the corrosion layer contains metal elements, mainly nickel (30.16%) and chromium (18.67%) from the coating as well as iron (10.23%) from the metal substrate, but it also contains important amounts of chlorine (19.32%) and oxygen (21.32%). These two layers (oxides formed on the metal substrate and the corrosion products of the NiCrAlY coating) suffered from attack by aggressive species like chlorine and oxygen. Figure 9(c) shows an intermediate part which corresponds to the bulk of corrosion layer; the EDS analysis showed that this layer is formed mainly by nickel (75.49%) and chromium (20.29%) from the sprayed NiCrAlY coating and by small amounts of oxygen (2.27%), iron (1.82%), and chlorine (0.07%). Figure 9(d) shows the corrosion products formed on the outer surface, which seems to be heterogeneous in

morphology as well as in chemical composition. Elemental analysis with EDS showed that this layer is formed mainly by two types of compounds: one of them conserves high contents from the original elements of the NiCrAlY coating (75.49% Ni and 20.29% Cr) and has very low contents of oxygen (2.27%), iron (1.82%), and chlorine (0.07%); the other compound contains much smaller amounts of nickel (10.93%) and chromium (3.63%) and the amounts of oxygen (26.78%), iron (50.13%), and chlorine (7.86%) are markedly increased.

The damage to the NiCrAlY coating at 700 °C for 11 h is due to the effects of chlorine. One of these effects is that it changes the morphology of the coating by the evaporation of metal chlorides leading to more rapid attack even if the amount of chlorides formed is negligible (Ref 21).

X-ray mapping for NiCrAlY coated on AISI 304 stainless steel at 700 °C, Fig. 10, indicates that the corrosion layer formed has different chemical compositions. In the most external part, aluminum and oxygen are detected, but high amounts of chlorine and iron are also found. In the whole layer nickel and iron are present, but higher concentrations of both elements are detected mainly in the central part of the layer. Diffusion of iron from substrate to the entire coating is also evident.

Important amounts of nickel, iron, and oxygen are also present near the substrate, which means that nickel-iron oxides have formed near the metal substrate.

X-ray mapping shows the absence of chromium in the entire scale; it can be explained by chromium volatilization or might be the EDS signal for Cr is overlapped with oxygen or other element so that Cr was not recognized.

X-ray mappings show that chlorine is present in the entire coating; the major role of Cl₂ is to destroy the protective oxide scale as well as to produce the internal voids by means of the chlorination-oxidation reactions. Cl₂ will dissolve into Cr₂O₃ and increase the cation-vacancy concentration and accelerate oxidation, or it will attack the alloy substructure and form metal chlorides (Ref 22). This leads to the formation of a porous (Fe, Ni) oxide scale, which is not protective, and the chlorine cycle of corrosion is not hindered. As a result, all the chromium of the coating is depleted, and chlorine may reach the steel through the interconnected pores and voids formed.

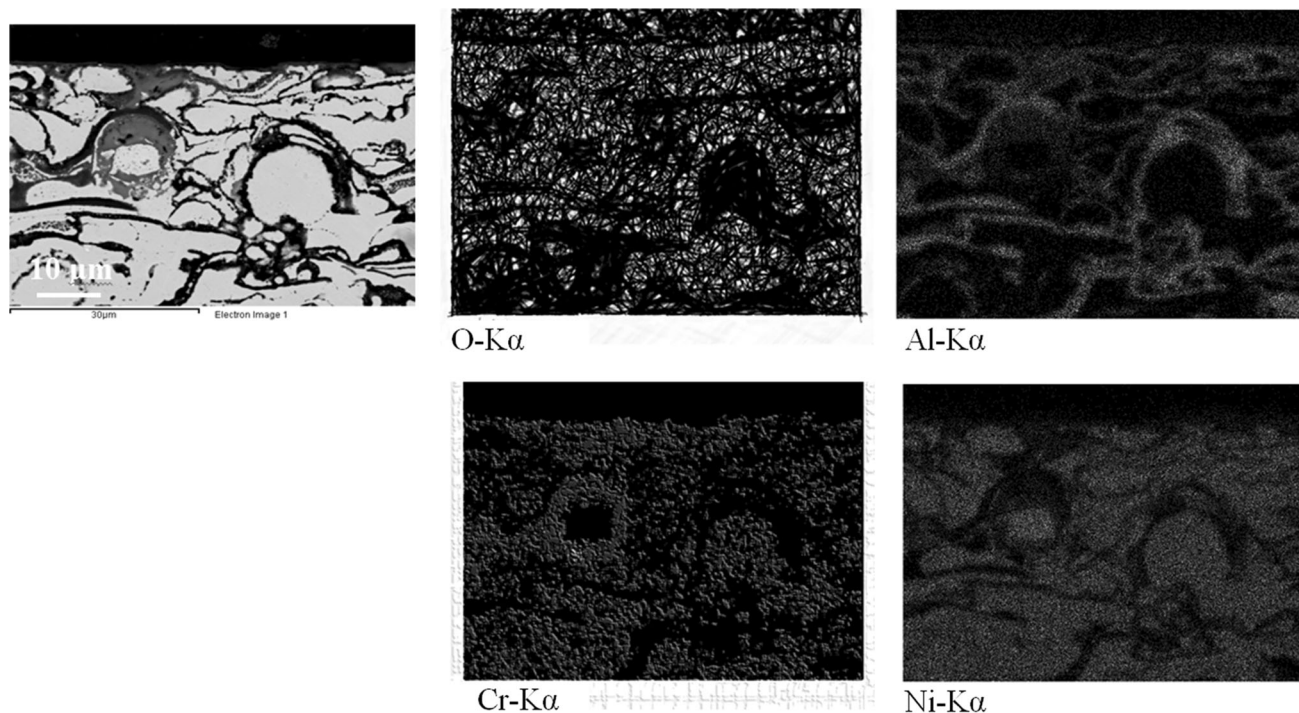


Fig. 8 Elements mapping of cross-section of NiCrAlY coating after 24 h at 650 °C in oxidation-chlorination atmosphere

As the protective feature of alumina scale has been deteriorated, oxygen and chlorine can easily penetrate into the coating and cause the formation of internal oxide and chromium oxychloride. This internal oxide and chromium oxychloride will accelerate the consumption of beneficial elements, and consequently speed up the corrosion process.

The oxidation-chlorination process can be described in detail as follows:

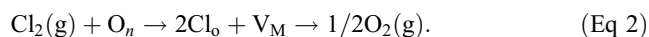
When NiCrAlY coating is exposed to an oxidizing environment at high temperature, the elements will gradually oxidize to thermodynamically stable oxides and form metal oxides. These oxides (Cr_2O_3 and Al_2O_3) provide a barrier for further diffusion of oxygen and other gaseous species. However, chlorine has the ability to penetrate the protective oxides. Cl_2 diffuses through the oxide, presumably through pores and cracks to the coating and coating metal interface, where it reacts with the metal alloy to form metal chloride.

Due to the high oxygen affinity of Y, it can be supposed that almost the whole amount of Y contained in the NiCrAlY powder will be oxidized during the flame-spraying process. The formation of Y oxides in the NiCrAlY coating during the deposition process would lead to a reduction in the amount of Y as a metallic component, and this means that only a small amount of Y is left to be oxidized during the high-temperature oxidation. Many authors reported on the transport of reactive elements ions in the alloy during oxidation, leading to the nucleation of oxide particles rich in RE in the oxide scale (Ref 23).

It is well known that RE additions prevent the formation of interfacial voids presumably by blocking outward diffusion of Al in the scales. RE may influence the collapse of dislocations loops at interfacial-vacancy aggregates, which maintains the interfacial cohesion and prevents cavity formation (Ref 24, 25). Segregation of sulfur contamination could also influence the formation of the interfacial voids. Because no sulfur could be detected as a segregant at the metal-scale interface, it was

assumed that the formation of the voids was due to the outward transport of aluminum and that the yttrium influence on the scale formation was minimal. In this work, Y has not been detected by EDS and XRD.

Chlorine alters the defect structure of the scale and increasing the diffusion coefficient of chloride ions by dissolving in the oxide scale (Ref 26). At ionic lattice sites, singly charged chloride ions may replace doubly charged oxygen ions. Considering charge and site balance, we have the following reaction (Ref 27, 28):



This reaction increases the concentration of cation vacancies. The vacancies tend to precipitate as voids resulting in pitting and spalling of the scale. The oxide scale cannot effectively hinder diffusion of the chloride ions through the scale to the matrix.

At the coating-metal interface, a very low oxygen potential exists (O_2 is consumed to produce metal oxides), at which volatile metal chlorides such as FeCl_3 and CrCl_2 are thermodynamically stable. The Cl_2 may react with metal according to the Reactions 1 to form metal chlorides:



Metal chloride has high vapor pressure at coating-metal interface and continuous evaporation may take place (Reaction 3):



The volatile metal chloride may diffuse through the oxidized coating. The oxygen concentration increases with increasing distance from the base metal, leading to oxidation of the metal chloride to solid metal oxide, according to the following reactions:

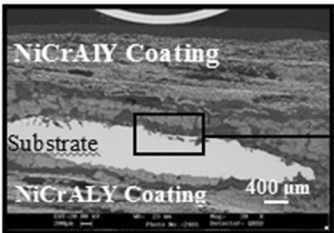
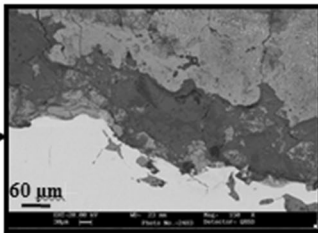
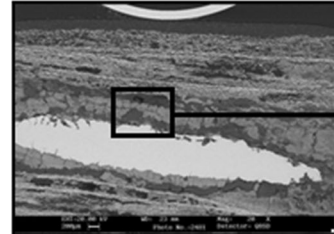
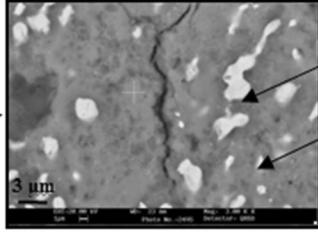
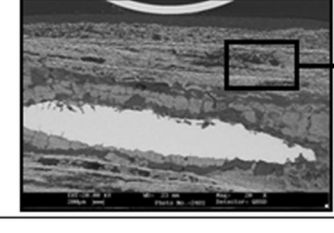
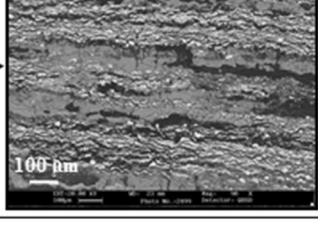
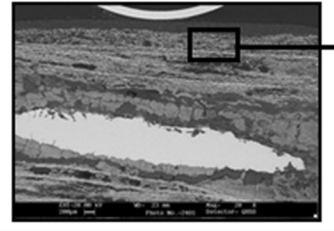
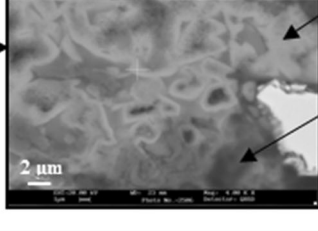
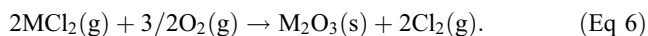
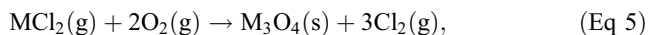
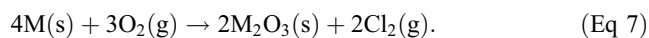
Interface	Studied Area	EDX Analysis
Metal/oxide interface 		30% Cl, 25.16% Ni, 23.65% O, 17.22% Al, 2.48% Fe, 0.35% Cr a) <u>Substrate interface</u>
substrate/coat interface 		Bright: 47.16%Ni, 46.84% Fe, 2.56% O, 2.54% Cr, 0.57% Cl Gray matrix: 30.16% Ni, 21.32% O, 19.34% Cl, 18.67% Cr, 10.23% Fe b) <u>Oxides scale on substrate</u>
Coat/oxide interface 		75.49% Ni%, 20.29 Cr%, 2.27 O%, Fe% 1.82, 0.07 Cl% c) <u>Corrosion damaged coating</u>
Coat/atmosphere interface 		Bright: 75.49% Ni, 20.29% Cr, 2.27% O, 1.82% Fe, and 0.00% Cl Gray: 50.13% Fe, 26.78% O, 10.93% Ni, 7.86% Cl, 3.63% Cr d) <u>Coating surface</u>

Fig. 9 SEM cross-section morphology with EDS analysis of NiCrAlY coat deposited on AISI 304 at 700 °C for 11 h in 1% Cl₂



The resulting oxides that precipitate from this gas phase reaction form a very loose metal-oxide layer, providing no protection by further attack. Thus, chlorine corrosion is often governed by linear corrosion rate. These oxides formed in this process are porous and non-protective. If oxidation of gaseous metal chlorides occurs near the metal surface, some of the chlorine released in the oxidation process will diffuse back to the base metal-oxide interface and the oxidation process will proceed.

According to Reactions 5 and 6, chlorine is released and can diffuse to the bulk gas or back to coating surface, and thus the cycle is formed. A graphical presentation of the corrosion mechanism is shown in Fig. 11. This cycle provides a continuous transport of metals away from the coating surface toward higher oxygen partial pressure with little net consumption of chlorides. The net reaction is thus



Gas diffusion through the scale is believed to be the rate-controlling step in the corrosion process.

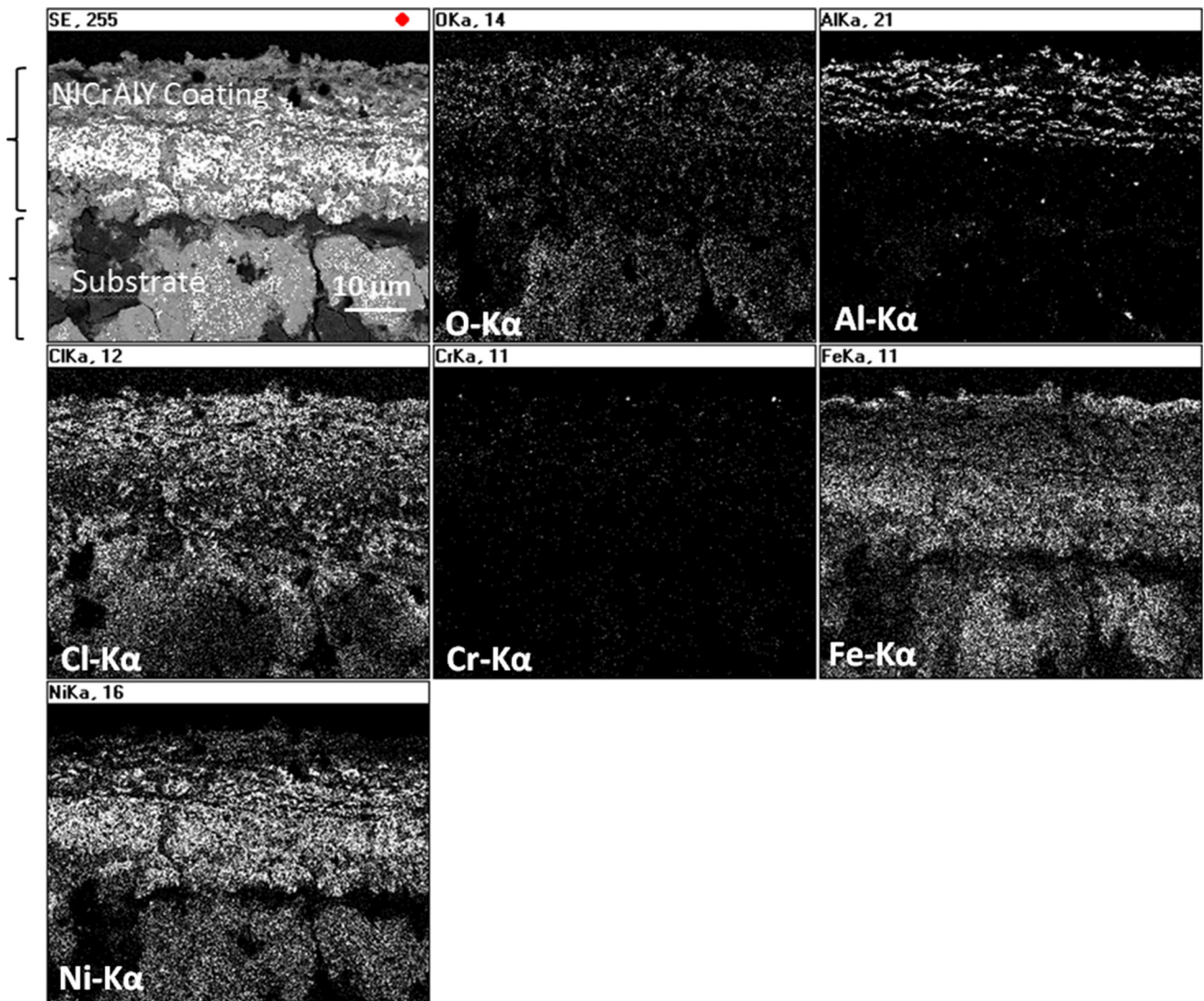


Fig. 10 X-ray mappings along the cross-section on NiCrAlY-coated AISI 304 in chlorine atmosphere during 11 h at 700 °C

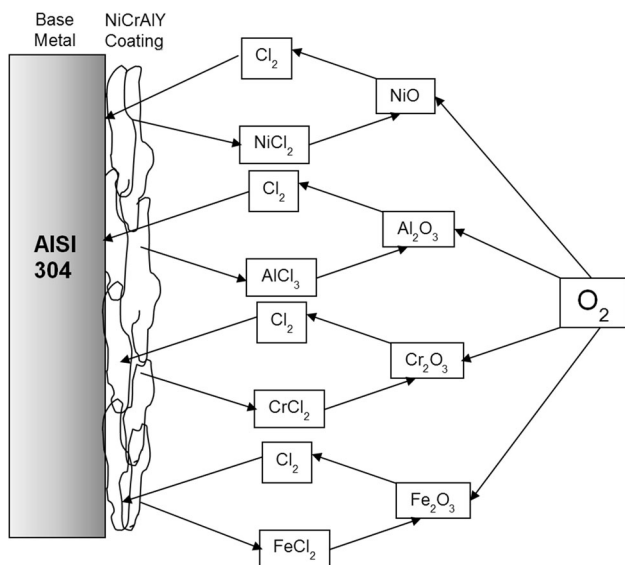
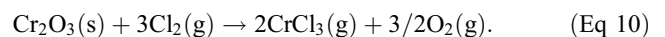
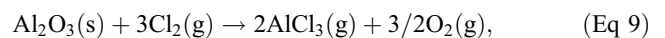
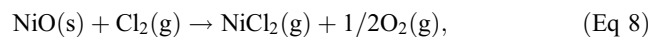


Fig. 11 Flow chart of oxychlorination of NiCrAlY coating on AISI 304

The oxide scale formed on NiCrAlY reacts with chlorine; the displacement reactions are



Transformation of metallic oxides into metallic chlorides in high temperature environments occur again giving place to further deterioration of oxide scale.

When chlorine has reached the metal surface, it reacts with metals forming metal chlorides. Gibbs free energies for metal chloride formation are strongly negative, which means that metal chlorides can form. The partial pressures of gaseous metal chlorides at 650 and 700 °C are significant and continuous evaporation of metal chlorides takes place in an open system. Gibbs free energies for metal chloride formation (and partial pressures of metal chlorides) at different temperatures (ranging from 550 to 850 °C) for Fe, Ni, Cr, and Al are presented in Table 2, extracted from results given but other authors (Ref 29-33).

Table 2 Formation reactions, Gibbs free energy for metal chlorides and oxides at different temperatures

Reactions	ΔG (kJ/mol)			
	600 °C	650 °C	700 °C	750 °C
Chlorination of metals				
Fe + Cl ₂ = FeCl ₂ (l)	-232	-227	-222	-218
Cr + Cl ₂ = CrCl ₂ (l)	-286	-280	-275	-268
Ni + Cl ₂ = NiCl ₂ (s)	-174	-167	-160	-153
Al + 3/2 Cl ₂ = AlCl ₃	-545	-540	-535	-532

A comparison of the Gibbs free energies of formation of the different divalent chlorides shows that the highest negative values correspond to CrCl₂ followed by FeCl₂ and NiCl₂ (Ref 22, 31). According to these data, a less reactive behavior is expected for nickel than for iron and chromium. The solid chlorides formed have considerable equilibrium vapor pressures $p_v(\text{Me}_x\text{Cl}_y)$ and therefore evaporate continuously and diffuse outward to the gas-scale interface.

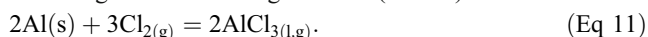
It can also be seen in Table 2 that Gibbs free energy for AlCl₃ formation is also very negative; therefore, this metal chloride can be formed at high temperatures (550-750 °C) under the experimental conditions.

The calculated partial pressures at 650 °C for oxygen $p_{\text{O}_2} = -0.19$ and chloride $p_{\text{Cl}_2} = -1.208$ and at 700 °C for oxygen $p_{\text{O}_2} = -0.166$ and chloride $p_{\text{Cl}_2} = -1.185$ indicate that iron and chromium chlorides are thermodynamically stable at these pressure conditions at both temperatures and the thermodynamically stable phase for aluminum at these partial pressures is Al₂O₃.

Besides, the Gibbs free energies for formation of Fe, Cr, Ni, and Al oxides are given in Table 2. All of these oxides have very negative values of Gibbs free energy indicating that Fe₂O₃, Fe₃O₄, Cr₂O₃, NiO₂, and Al₂O₃ can form in the range of temperatures in this study. The more negative Gibbs free energy for formation of Al₂O₃ can explain the formation of this oxide in the NiCrAlY coating in the experimental conditions at 650 °C (Ref 22, 31, 33).

The actual oxygen and chlorine potentials prevailing at the scale/metal interface will differ a lot from those in the atmosphere, due to the additional reactions between chlorine and metals and between chlorides and oxygen.

Considering that chlorine penetrates into the scale faster than oxygen and enriches at the scale/metal interface, the oxygen pressure at the scale/metal interface will be fixed by the local equilibrium established between the oxides and the metals. In consequence, besides FeCl₂ and CrCl₂, AlCl₃ becomes stable too; the Cr and Al chlorides will rapidly evaporate and diffuse outward through the scale by vapor-phase transport, and are decomposed into oxides again as they reach zones in the scale with higher partial pressures of oxygen. The CrCl₂ can then be oxidized to form Cr₂O₃ and the Cl₂; this latter diffuses inward to attack again the metal at the scale/metal interface. If the temperature is higher, volatilization of CrCl₂ is preponderant and the scale can be Cr depleted (Ref 22, 30-34). If oxygen and chlorine pressure are low enough, the AlCl₃ is a stable phase and formation of Al₂O₃ is hindered. Therefore, Al will be selectively removed from the coating as chloride according to the following reaction (Ref 30):



The AlCl₃ will diffuse outward due to its high volatility and be transferred into aluminum oxides subsequently at the outer part of the coating (scale). In these circumstances, aluminum moves toward to the outer surface of the coating.

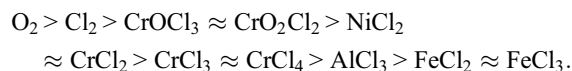
Moreover, at these partial pressures and due to the enhanced iron and chromium activity and enriched chlorine, strong outward transport of FeCl₂ and CrCl₂ will occur leading to rapid transport of iron as iron oxide layer due to decomposition of the chloride to oxide and depletion of chromium due to high volatilization of CrCl₂.

Finally, the enhanced internal penetration rate of oxygen is unlikely to be caused just by solid diffusion in the bulk coating or even by grain boundary diffusion. Instead, several other key factors should be considered. First, the diffusivity and solubility of atomic chlorine dissolved in the coating can be much higher than that of oxygen. In this circumstance, the formation of AlCl₃ at the corrosion front is well favored and its outward diffusion will produce a void-rich porous region beneath the surface scale, which can act as open channels for the subsequent fast inward transport of oxygen (Ref 30, 33).

The preformed aluminum oxide is attacked by chlorine at 700 °C and thus the other metallic elements of the coating can be exposed to corrosive gas environment. The chlorine gas can diffuse into the interface between metal and preformed oxide through the oxide film and then follows the active oxidation steps as described: (1) diffusion of chlorine through preformed aluminum oxide and microdefects of the oxide where the oxygen potential is low, (2) reaction of the chlorine with aluminum in the alloy, (3) formation of the volatile aluminum chloride (Eq 11), (4) diffusion of the volatile aluminum chloride, AlCl₃, through defects of the coatings through making cracks or holes due to the high vapor pressure of the volatile metal chloride, (5) formation of chlorine and aluminum oxide from the reaction between aluminum chloride and oxygen, (Eq 9), and (6) transport of some parts of the gaseous aluminum chloride to the bulk gas phase.

In previous investigations (Ref 35), the experimental gas components (O₂ and Cl₂) are shown to be the species with the highest diffusion coefficients. Among these two species, O₂ diffuses more rapidly; the diffusion coefficient at 1000 K for O₂ is 1.55 cm²/s, while at the same temperature Cl₂ diffuses with 0.96 cm²/s in the gas mixture.

Metal chlorides diffuse more slowly, and differences may be noticed in the diffusion coefficients between species not only as a function of their metallic element, but also as a function of their number of chlorine and oxygen atoms. For a general view of the diffusivities of each species, the following order is developed (species are ordered according to their diffusivities from the fastest to the slowest, Ref 35):



With this comparison, chromium chlorides and nickel chlorides are shown to be the fastest species among the metal chlorides, followed by the aluminum chlorides, and finally the iron chlorides. At 727 °C, the diffusion coefficients range from 0.823 cm²/s for CrO₂Cl₂ to 0.451 cm²/s for FeCl₃. It should be noted that the difference in the diffusivities of the species is accentuated by increasing the temperature.

Active oxidation was responsible for the accelerated corrosion oxidizing environments. The coating and substrate AISI

304 were prone to chlorine attack in both atmospheres through oxide network at splat boundaries.

Breakdown corrosion at 700 °C is caused by dissolution of Cr₂O₃ and Al₂O₃. In addition, corrosive O and Cl diffused inward along the grain boundary of the coating. With time increasing, the coating was corroded completely and lost protection rapidly. In fact, its corrosion behavior represents that of the substrate alloy at last stage.

4. Conclusions

1. NiCrAlY coating deposited by (OF) thermal spraying shows a severe temperature dependence concerning its corrosion resistance in chlorine plus air environment.
2. The high temperature chlorination resistance of NiCrAlY coating at 650 °C for 24 h has been attributed to the formation of chromium oxides and nickel-chromium at the surface coating, and alumina at the splat boundaries. The oxide scale has been preferentially formed at the splat boundaries due to oxidation of the active elements of the coating. The Ni-Cr metallic-rich phase of the coating mostly remains in the un-oxidized state.
3. At 700 °C the corrosion behavior reaches the breakdown limit at 11 h. Therefore, the behavior moves from parabolic to linear as a result of the formation of porous and cracked oxides: β-Fe₂O₃, Fe₂O₃, etc. The EDS study of the cross-section of the degraded samples at 700 °C indicated that the mechanism of corrosion corresponds to active oxidation due to the selective diffusion of chlorine to the surface with the formation of voids below and the depletion of chromium compounds at the surface.
4. The good resistance of the heat-treated NiCrAlY coating at 650 °C in a 1% Cl₂ atmosphere suggests that the OF thermal spraying process can be used as a technological alternative to more expensive vacuum plasma spray and high velocity OF deposition.

References

1. S. Paul and M.D.F. Harvey, Corrosion Testing of Ni alloy HVOF Coatings in High Temperature Environments for Biomass Applications, *J. Therm. Spray Technol.*, 2013, **22**(2-3), p 316–327
2. D.P. Whittle, D. Coutsouradis, P. Felix, H. Fischmeister, L. Habraken, Y. Linblon, and M.O. Speidel, Ed., *High Temperature Alloys for Gas Turbines*, Applied Science, London, 1978, p 109
3. F. Wang, X. Tian, Q. Li, L. Li, and X. Peng, Oxidation and Hot Corrosion Behaviour of Sputtered Nanocrystalline Coatings of Superalloy K52, *Thin Solid Films*, 2008, **516**(6), p 5740–5747
4. D. Mudgal, S. Sigh, and S. Prakash, Hot Corrosion Behavior of Some Superalloys in a Simulated Incinerator Environment at 900°C, *J. Mater. Eng. Perform.*, 2014, **23**(1), p 238–249
5. D. Xie, Y. Xiong, and F. Wang, Effect of an Enamel Coating on the Oxidation and Hot Corrosion Behaviour of a HVOF-Sprayed Co-Cr-Al-Y Coating, *Oxid. Met.*, 2003, **59**(5-6), p 503–516
6. D. Wolfe and J. Singh, Functionally Gradient Ceramic/Metallic Coatings for Gas Turbine Components by High-Energy Beams for High-Temperature Applications, *J. Mater. Sci.*, 1998, **33**, p 3677–3692
7. W. Brandl, D. Toma, and H.J. Grabke, The Characteristic of Alumina Scales Formed on HVOF-Sprayed MCrAlY Coatings, *Surf. Coat. Technol.*, 1998, **108**(109), p 10–15
8. W. Brandl, H.J. Grabke, D. Toma, and J. Kruger, The Oxidation Behaviour of Sprayed MCrAlY Coatings, *Surf. Coat. Technol.*, 1996, **86**(87), p 41–47
9. M. Schutze, M. Malessa, V. Rohr, and T. Weber, Development of Coatings for Protection in Specific High Temperature Environment, *Surf. Coat. Technol.*, 2006, **201**(7), p 3872–3879
10. M.A. Uusitalo, P.M.J. Vuoristo, and T.A. Mantyla, High Temperature Corrosion of Coatings and Boiler Steels Below Chlorine-Containing Salt Deposits, *Corros. Sci.*, 2004, **46**(6), p 1311–1331
11. A. Hernas, M. Imosa, B. Formanek, and J. Cizner, High Temperature Chlorine-Sulfur Corrosion of Heat Resisting Steels, *J. Mater. Process. Technol.*, 2004, **157-158**, p 348–353
12. A. Pardo, M.C. Merino, A.E. Coy, F. Viejo, R. Arrabal, and E. Matykina, Corrosion Behaviour of Magnesium/Alumina Alloys in 3.5 wt% NaCl, *Corros. Sci.*, 2008, **50**(3), p 823–834
13. M. Spiegel, Salt Melt Induced Corrosion of Metallic Materials in Waste Incineration Plants, *Mater. Corros.*, 1999, **50**(7), p 373–393
14. H.H. Krause and I.G. Wright, Boiler Tube Failure in Municipal Waste-to-Energy Plants, *Mater. Perform.*, 1996, **35**(1), p 46–53
15. A. Zahs, M. Spiegel, and H.J. Grabke, Chloridation and Oxidation of Iron, Chromium, Nickel and their Alloys in Chloridizing and Oxidizing Atmospheres at 400–700°C, *Corros. Sci.*, 2000, **42**(6), p 1093–1122
16. K.A. Habib, J.J. Saura, C. Ferrer, and M.S. Damra, Comparison of Flame Sprayed Al₂O₃/TiO₂ Coatings: Their Microstructure, Mechanical Properties and Tribology Behaviour, *Surf. Coat. Technol.*, 2006, **201**, p 1436–1443
17. K.A. Habib, J.J. Saura, C. Ferrer, M.S. Damra, and I. Cervera, Oxidation Behaviour at 1123 K of AISI, 304-Ni/Al-Al₂O₃/TiO₂ Multilayer System Deposited by Flame Spray, *Rev. Metal.*, 2011, **47**(2), p 126–137
18. K.A. Habib, M.S. Damra, J.J. Carpio, I. Cervera, and J.J. Saura, Oxidation Behaviour of a NiCrAlY Coating Deposited on AISI 304 and AISI 316 Stainless Steels by Flame Thermal Spraying Technique (Oxyfuel OF), Presented at the 8th High Temperature International Conference on Corrosion and Protection of Materials (HTCPM8), Les Embiez-France, May 20-25, 2102
19. G.Y. Lai, *High-Temperature Corrosion of Engineering Alloys*, ASM International, Materials Park, OH, 1990, p 85–115
20. Y.N. Wua, M. Qin, Z.C. Feng, Y. Liang, C. Suna, and F.H. Wang, Improved Oxidation Resistance of NiCrAlY Coatings, *Mater. Lett.*, 2003, **57**, p 2404–2408
21. G. Sorell, The Role of Chlorine in High Temperature Corrosion in Waste-to-Energy Plants, *Mater. High Temp.*, 1997, **14**(3), p 207–220
22. C.J. Wang and T.T. He, Morphological Development of Subscale Formation in Fe-Cr(Ni) Alloys with Chloride and Sulfates Coating, *Oxid. Met.*, 2002, **58**(3-4), p 415–437
23. D. Toma, W. Brandl, and U. Köster, Studies on the Transient Stage of Oxidation of VPS and HVOF Sprayed MCrAlY Coatings, *Surf. Coat. Technol.*, 1999, **120-121**, p 8–15
24. D. Toma, W. Brandl, and U. Köster, The Characteristics of Alumina Scales Formed on HVOF-Sprayed MCrAlY Coatings, *Oxid. Met.*, 2000, **53**(1/2), p 125–137
25. B.A. Pint, Experimental Observations in Support of the Dynamic-Segregation Theory to Explain the Reactive-Element Effect, *Oxid. Met.*, 1996, **45**(1-2), p 1–37
26. B.R. Singh and P. Balk, Oxidation of Silicon in the Presence of Chlorine and Chlorine Compounds, *J. Electrochem. Soc.*, 1978, **125**(3), p 453–461
27. R. Subramanian, R. Dieckmann, G. Eriksson, and A. Pelton, Model Calculations of Phase Stabilities of Oxide Solid Solutions in Co-Fe-Mn-O System at 1200°C, *Phys. Chem. Solids*, 1994, **55**(5), p 391–404
28. N. Kanari, D. Mishra, J. Mochón, L.F. Vereja, F. Doit, and E. Allain, Algunos aspectos Cineticos de las Reacciones de Solidos con Cloro, *Rev. Metal.*, 2010, **46**(1), p 22–36 (in Spanish)
29. M.A. Uusitalo, P.M.J. Vuoristo, and T.A. Mäntylä, High Temperature Corrosion of Coatings and Boiler Steels Below Chlorine-Containing Salt Deposits, *Corros. Sci.*, 2004, **46**, p 1311–1331
30. G. Han and W.D. Cho, High-Temperature Corrosion of Fe₃Al in 1% Cl₂/Ar, *Oxid. Met.*, 2002, **58**(3/4), p 391–413
31. A. Zahs, M. Spiegel, and H.J. Grabke, Chloridation and Oxidation of Iron, Chromium, Nickel and Their Alloys in Chloridizing and Oxidizing Atmospheres at 400–700°C, *Corros. Sci.*, 2000, **42**, p 1093–1122
32. Y. Yonghua Shu, F. Wang, and W. Wu, Corrosion Behavior of Pure Cr with a Solid NaCl Deposit in O₂ Plus Water Vapor, *Oxid. Met.*, 2000, **54**(5/6), p 457–471

33. C.J. Wang and C.C. Li, The High-Temperature Corrosion of Austenitic Stainless Steel with a NaCl Deposit at 850°C, *Oxid. Met.*, 2004, **61**(5/6), p 485–505
34. M.C. Mayoral, J.M. Andrés, J. Belzunce, and V. Higuera, Study of Sulphidation and Chlorination on Oxidized SS310 and Plasma-Sprayed Ni-Cr Coatings as Simulation of Hot Corrosion in Fouling and Slagging in Combustion, *Corros. Sci.*, 2006, **48**, p 1319–1336
35. H. Latreche, S. Doublet, and M. Schütze, Development of Corrosion Assessment Diagrams for High Temperature Chlorine Corrosion Part II: Development of “Dynamic” Quasi-stability Diagrams, *Oxid. Met.*, 2009, **72**, p 31–65